

ISO observations of far-infrared rotational emission lines of water vapor toward the supergiant star VY Canis Majoris *

David A. Neufeld¹, Helmut Feuchtgruber², Martin Harwit³, and Gary J. Melnick⁴

¹ Department of Physics & Astronomy, The Johns Hopkins University, 3400 North Charles Street, Baltimore, MD 21218

² Max-Planck Institut für extraterrestrische Physik, Postfach 1603, D-85740, Garching, Germany

³ 511 H Street S.W., Washington, DC 20024-2725; also Cornell University

⁴ Harvard-Smithsonian Center for Astrophysics, 60 Garden Street, Cambridge, MA 02138

* Based on observations with ISO, an ESA project with instruments funded by ESA Member States (especially the PI countries: France, Germany, the Netherlands and the United Kingdom) with the participation of ISAS and NASA.

Subject headings: circumstellar matter – infrared: stars – stars: abundances – supergiants – molecular processes – stars: individual (VY Canis Majoris)

ABSTRACT

We report the detection of numerous far-infrared emission lines of water vapor toward the supergiant star VY Canis Majoris. A $29.5 - 45 \mu\text{m}$ grating scan of VY CMa, obtained using the Short Wavelength Spectrometer (SWS) of the Infrared Space Observatory (ISO) at a spectral resolving power $\lambda/\Delta\lambda$ of approximately 2000, reveals at least 41 spectral features due to water vapor that together radiate a total luminosity $\sim 25 L_{\odot}$. In addition to pure rotational transitions within the ground vibrational state, these features include rotational transitions within the (010) excited vibrational state. The spectrum also shows the ${}^2\Pi_{1/2}(J = 5/2) \leftarrow {}^2\Pi_{3/2}(J = 3/2)$ OH feature near $34.6 \mu\text{m}$ in absorption. Additional SWS observations of VY CMa were carried out in the instrument's Fabry-Perot mode for three water transitions: the $7_{25} - 6_{16}$ line at $29.8367 \mu\text{m}$, the $4_{41} - 3_{12}$ line at $31.7721 \mu\text{m}$, and the $4_{32} - 3_{03}$ line at $40.6909 \mu\text{m}$. The higher spectral resolving power $\lambda/\Delta\lambda$ of approximately 30,000 thereby obtained permits the line profiles to be resolved spectrally for the first time and reveals the "P Cygni" profiles that are characteristic of emission from an outflowing envelope.

1. Introduction

A wealth of recent data from the Infrared Space Observatory (ISO; Kessler et al. 1996) has demonstrated that water vapor is a ubiquitous constituent of the astrophysical universe. With its powerful spectroscopic capability unhindered by atmospheric absorption and covering the $2.38 - 197 \mu\text{m}$ spectral region without interruption, ISO has detected water vapor in astrophysical environments as diverse as star-forming interstellar clouds (e.g. van Dishoeck & Helmich 1996; Helmich et al. 1996; Ceccarelli et al. 1998; van Dishoeck et al. 1998); Herbig Haro objects (Liseau et al. 1996); shocked interstellar regions (e.g. Harwit et al. 1998); the atmospheres of Jupiter, Saturn, Uranus, Neptune and Titan (Feuchtgruber et al. 1997; Lellouch et al. 1997; Coustenis et al. 1998); the photospheres of cool stars (e.g. Tsuji et al. 1997); and the circumstellar outflows from oxygen-rich evolved stars (e.g. Neufeld et al. 1996; Barlow et al. 1996, Justtanont et al. 1996).

The data now available from ISO observations support earlier theoretical predictions of a substantial abundance of water vapor within warm molecular astrophysical environments where the elemental abundance of oxygen exceeds that of carbon. Since the water molecule possesses a large dipole moment, water rotational transitions play an important role in the thermal balance of the gas (e.g. Neufeld, Lepp & Melnick 1995).

As part of a program to study water vapor in shocked interstellar regions and circumstellar outflows, we have carried out a search for far-infrared rotational emissions from water toward VY CMa, a high-mass red supergiant of spectral type M5Iae that is believed to be in an advanced stage of evolution with a bolometric luminosity $\sim 5 \times 10^5 L_{\odot}$ and a mass loss rate that exceeds $10^{-4} M_{\odot} \text{yr}^{-1}$ (Danchi et al. 1994). A complete spectrum of VYCMa covering the 2.38 to $45 \mu\text{m}$ spectral region was obtained using the Short Wavelength Spectrometer (SWS; de Graauw et al. 1996) on board ISO and will be presented in a future publication; in this Letter we consider only the 29.5 - $45 \mu\text{m}$ region (SWS Band 4) that contains the strongest rotational emissions from water.

2. Observations

All the observations of VY CMa reported here were carried out using the SWS instrument. A complete spectrum covering the 2.38 to $45 \mu\text{m}$ spectral region was obtained using the instrument's grating mode at a spectral resolving power $\lambda/\Delta\lambda \sim 1000 - 2500$ (the 29.5 - $45 \mu\text{m}$ portion of which is presented here.) In addition, the spectra of three rotational lines of ortho-water were obtained in Fabry-Perot (FP) mode at a spectral resolving power $\lambda/\Delta\lambda \sim 3 \times 10^4$: the $7_{25} - 6_{16}$ line at $29.8367 \mu\text{m}$, the $4_{41} - 3_{12}$ line at $31.7721 \mu\text{m}$, and the $4_{32} - 3_{03}$ line at $40.6909 \mu\text{m}$.

The observations were all carried out on 1997 November 19 (grating scan) and 1997 November 20 (FP scans) with the ISO beam centered at position $\alpha = 7^{\text{h}}22^{\text{m}}58.3^{\text{s}}$, $\delta = -25^{\circ}46'03''$. The beam size was $20 \times 33''$ for the grating scan and $17 \times 40''$ for the FP scan. Including overheads for dark current measurements and calibration, the total observing times on target were 10185 s for the

complete $2.38 - 45 \mu\text{m}$ grating scan and 3962 s for the three Fabry-Perot scans.

3. Results

The reduction of the grating spectrum was carried out using the SWS Interactive Analysis system, applying calibration files from version 7.0 of the ISO pipeline software. The Fabry-Perot spectra were initially reduced using version 6.22 of the ISO pipeline software, and the ISAP software package¹ was then used to remove bad data points and to co-add the individual spectral scans.

The $29.5 - 45 \mu\text{m}$ grating scan of VY CMa, shown in Figure 1, reveals a strikingly rich spectrum of water rotational transitions. At least 41 features are readily identifiable as water, corresponding to a density of more than 2 such features per micron of wavelength coverage. Line identifications and flux estimates are given in Table 1. Here we have been quite conservative in identifying spectral features with water transitions, including only those features for which the identification seems most secure.

The flux calibration is believed accurate to $\sim 30\%$, and the typical 1σ statistical error in the flux is $\sim \text{several} \times 10^{-20} \text{ W cm}^{-2}$. Multiple scans of some portions of the spectrum strongly suggest that all features apparent to the eye are real. However, many features, whether in absorption or emission, are still not reliably identified (although many of them may, in fact, be water vapor lines). As a result, the proper identification of a baseline, on top of which individual features are observed, is quite uncertain. For many water lines, this difficulty substantially increases the uncertainties in the line flux estimates given in Table 1.

In addition to transitions within the ground vibrational state, the line list in Table 1 includes rotational transitions within the (010) excited vibrational state. Two radio wavelength transitions within the (010) state had previously been detected in VY CMa by Menten & Melnick (1989).

The only molecule other than water for which a feature has been identified in this spectral region is OH, the primary photodissociation product of water, which we detected by means of the $^2\Pi_{1/2}(J = 5/2) \leftarrow ^2\Pi_{3/2}(J = 3/2)$ absorption feature at $34.6 \mu\text{m}$.

Several broad spectral features have been identified in the $20 - 45 \mu\text{m}$ spectra of other evolved stars (e.g. Waters et al. 1996), some of which have been tentatively attributed to crystalline silicates. One broad spectral feature is prominent in the $29.5 - 45 \mu\text{m}$ VY CMa spectrum (Figure 1). It is centered at wavelength $30.4 \pm 0.1 \mu\text{m}$, with a width $\sim 0.5 \mu\text{m}$, and a peak flux lying $\sim 3\%$ above the continuum. A feature with very similar properties has been detected in each of the sources NML Cyg, AFGL 4106, HD 179821 and NGC 6302 (Waters et al. 1996): its identification is unknown at present.

¹The ISO Spectral Analysis Package (ISAP) is a joint development by the LWS and SWS Instrument Teams and Data Centers. Contributing institutes are CESR, IAS, IPAC, MPE, RAL and SRON.

Figure 2 shows the Fabry-Perot spectra obtained toward VY CMa. The corresponding line fluxes are listed in Table 2: once again, the likely errors in the flux calibration are believed to be $\sim 30\%$.

4. Discussion

4.1. Grating spectrum

The grating spectrum of VY CMa shown in Figure 1 demonstrates dramatically the ubiquitous nature of water vapor emission lines in the far-infrared spectral region. Adopting 1500 pc as the most credible estimate of the distance to VY CMa (Lada & Reid 1978), we find that the identified water features listed in Table 1 carry a total luminosity of $25 L_{\odot}$. Detailed modeling of the water line fluxes, which we defer to a later publication, will be complicated significantly by large departures from spherical symmetry. In particular, recent Hubble Space Telescope observations of VY CMa (Kastner & Weintraub 1998) vividly demonstrate the highly anisotropic nature of the surrounding outflow. These observations suggest that a highly flattened circumstellar envelope obscures the photosphere of VY CMa from direct view along our line of sight, but that photospheric radiation does leak out along other directions, giving rise to an elongated reflection nebula. Clearly, this complex geometry is very different from the idealized spherical geometry that has been assumed previously in modeling water emissions from circumstellar outflows (e.g. Deguchi & Rieu 1990, Chen & Neufeld 1995). We expect that future modeling efforts will be usefully constrained by additional observations of the water vibrational bands near 2.7 and $6.2 \mu\text{m}$ and of rotational absorption lines in the $16 - 19.5 \mu\text{m}$ spectral region, the reduction and analysis of which are underway.

The strength of the $34.6 \mu\text{m}$ OH absorption feature is of relevance to models for the radiative pumping of 1612 MHz OH masers by $34.6 \mu\text{m}$ infrared radiation (e.g. Elitzur, Goldreich & Scoville 1976). The OH absorption that we observed presumably arises in a shell surrounding the source where the outflowing water vapor is photodissociated by the interstellar radiation field. Assuming spherical symmetry, we find that the total rate of absorption in the OH $34.6 \mu\text{m}$ feature is 1.0×10^{47} photons per second (for an assumed distance to the source of 1500 pc). The average maser photon emission rate is $4.3 \times 10^{45} \text{ s}^{-1}$ (Harvey et al. 1974), with a typical time variability $\lesssim 20\%$. Disregarding the complications introduced by anisotropy, we therefore find that ~ 23 photons are absorbed in the $34.6 \mu\text{m } ^2\Pi_{1/2}(J = 5/2) \leftarrow ^2\Pi_{3/2}(J = 3/2)$ line for every 1612 MHz maser photon emitted. The ratio of $34.6 \mu\text{m}$ photons absorbed to 1612 MHz photons emitted is somewhat higher than the value of 14 reported by Sylvester et al. (1997) for the evolved star of IRC+10420.

4.2. Fabry-Perot spectra of VY CMa

The Fabry-Perot spectra of VY CMa shown in Figure 2 are of sufficiently high spectral resolution to yield useful information about the line profile. As far as we are aware, these are the first spectra in which the line profiles of thermal water emissions from a circumstellar outflow have been resolved spectrally. All three observed lines exhibit the classic “P Cygni” profiles associated with line formation in an outflow. We find that the observed line profiles are consistent with the line emission expected from a spherical outflow at constant velocity, v_{out} , accompanied by continuum emission that suffers blueshifted absorption in the approaching side of the outflow. Figure 2 shows that an outflow velocity of $v_{\text{out}} = 25 \text{ km s}^{-1}$ yields an acceptable fit for all three lines: here the dashed line represents the symmetric, parabolic emission line profile expected for optically-thick line emission from a constant velocity outflow; the dotted line represents continuum radiation with an optically-thick absorption feature blueshifted by velocity v_{out} relative to the emission line; and the solid line represents the sum of those components after convolution with the instrumental profile.

The integrated fluxes in the emission and absorption features, the equivalent widths of the absorption features, and the emission line velocity relative to the LSR, v_E , are all tabulated in Table 2. The values of v_E are in acceptable agreement with each other and with the stellar LSR velocity of $\sim 18 \text{ km s}^{-1}$ inferred for this source (Reid & Dickenson 1976). The value of 25 km s^{-1} obtained for v_{out} is close to – but somewhat smaller than – the estimates of $\sim 37 \text{ km s}^{-1}$ and $\sim 32 \text{ km s}^{-1}$ inferred previously for the terminal outflow velocity from observations of the thermal $J = 2 - 1$ line of SiO (Reid & Dickenson 1976) and the 1612 MHz OH maser line (Reid & Muhleman 1978). The observed spectra therefore provide an important observational confirmation of theoretical predictions (e.g. Deguchi & Rieu 1990, Chen & Neufeld 1995) that the far-infrared water line emission detected from circumstellar outflows is generated largely within a region where the outflow has already reached – or nearly reached – its terminal velocity. The absorption line equivalent width is considerably larger for the $4_{32} - 3_{03}$ line at $40.6909 \mu\text{m}$ than for the other two lines, a difference that presumably results from a large optical depth in this transition which has a lower state of energy, E_l/k , only 197 K.

It is a pleasure to acknowledge the support provided by the Infrared Processing and Analysis Center (IPAC). We also thank members of the help desk at Vilspa for their assistance. We gratefully acknowledge the support of NASA grants NAG5-3316 to D.A.N.; NAG5-3347 to M.H.; and NAG5-3542 and NASA contract NAS5-30702 to G.J.M. M.H. also thanks the Alexander von Humboldt foundation and the Max Planck Institute for Radioastronomy for their hospitality during a three-month visit to the MPIfR in Bonn.

REFERENCES

Barlow, M.J., et al. 1996, A&A, 315, L241

- Ceccarelli, C., et al. 1998, A&A, 331, 372
- Chen, W., & Neufeld, D.A. 1995, ApJ, 452, L99
- Clegg, P.E., et al. 1996, A&A, 315, L38
- Coustenis, A., et al. 1998, A& A, 336, L85
- de Graauw, T., et al. 1996, A&A, 315, L49
- Danchi, W.C., Bester. M., Degiacomi, C.G., Greenhill, L.J., & Townes, C.H. 1994, AJ, 107, 1469
- Deguchi, S., & Rieu, N. 1990, ApJ, 360, L27
- Diamond, P.J., Norris, R.P., & Booth, R.S. 1984, MNRAS, 207, 611
- Elitzur, M., Goldreich, P., & Scoville, N. 1976, ApJ, 205, 384
- Feuchtgruber, H., Lellouch, E., de Graauw, T., Encrenaz, T., & Griffin, M. 1997, Nature, 389, 159
- Goldreich, P., & Scoville, N. 1976, ApJ, 205, 144
- Harvey, P.M., Bechis, K.P., Wilson, W.J., & Ball, J.S. 1974, ApJS, 27, 331
- Helmich, F.P., et al. 1996, A&A, 315, L173
- Justtanont, K., et al. 1996, A&A, 315, L217
- Kastner, J.H., & Weintraub, D.A. 1998, AJ, 115, 1592
- Kessler, M., et al. 1996, A&A, 315, L27
- Harwit, M., Neufeld, D.A., Melnick, G.J., & Kaufman, M. 1998, ApJ, 497, L105
- Lellouch, E., Feuchtgruber, H., De Graauw, T., Bezard, B., Encrenaz, T, & Griffin, M. 1997, “First ISO Workshop on Analytical Spectroscopy”, ESA, SP-419, p. 131
- Lada, C.J., & Reid, M.J. 1978, ApJ, 219, 95
- Liseau, R., et al. 1996, A&A, 315, L181
- Menten, K.M., & Melnick, G.J. 1989, ApJ, 341, L91
- Neufeld, D.A., Lepp, S., & Melnick, G.J. 1995, ApJS, 100, 132
- Neufeld, D.A., et al. 1996, A&A, 315, L237
- Reid, M.J., & Dickenson, D.F. 1976, ApJ, 207, 784
- Reid, M.J., & Muhleman, D.O. 1978, ApJ, 220, 229

- Richards, A.M.S., Yates, J.A., & Cohen, R.J. 1996, MNRAS, 282, 665
- Sylvester, R.J., et al. 1997, MNRAS, 291, L42
- Toth, R. A. 1991, J Opt Soc Am B, 8, 2236
- Tsuji, T., Ohnaka, K., Aoki, W., & Yamamura, I. 1997, A&A, 320, L1
- van Dishoeck, E.F. & Helmich, F.P. 1996, A&A, 315, L177
- van Dishoeck, E.F., et al. 1998, ApJ, 502, L173
- Waters, L.B.F.M., et al. 1996, A&A, 315, L361

TABLE 1
Lines identified in the grating scan of VY CMa

| Line | Wavelength (μm) | Upper state Energy (E/k) (K) | Flux ($10^{-18} \text{ W cm}^{-2}$) |
|--|---------------------------------|------------------------------------|--|
| H ₂ O 7 ₆₁ – 6 ₅₂ | 30.526 | 1750 | 0.91 |
| H ₂ O 7 ₆₂ – 6 ₅₁ | 30.529 | 1750 | — ^a |
| H ₂ O 4 ₄₁ – 3 ₁₂ | 31.772 | 702 | 0.65 |
| H ₂ O 6 ₄₃ – 6 ₁₆ | 32.313 | 1089 | 0.88 |
| H ₂ O 7 ₅₂ – 6 ₄₃ | 32.991 | 1525 | 2.22 |
| H ₂ O 6 ₆₀ – 5 ₅₁ | 33.005 | 1504 | — ^a |
| H ₂ O 6 ₆₁ – 5 ₅₀ | 33.005 | 1504 | — ^a |
| H ₂ O 10 ₄₇ – 9 ₃₆ | 33.510 | 2275 | 0.90 |
| H ₂ O 5 ₅₀ – 5 ₂₃ | 33.833 | 1068 | 0.82 |
| H ₂ O 9 ₄₆ – 8 ₃₅ | 34.396 | 1929 | 0.68 |
| H ₂ O 7 ₃₄ – 6 ₂₅ | 34.549 | 1212 | 0.58 |
| OH $J = 5/2- \leftarrow 3/2+^b$ | 34.603 | 416 | –1.49 |
| OH $J = 5/2+ \leftarrow 3/2-^b$ | 34.629 | 415 | –0.61 |
| H ₂ O 7 ₄₃ – 6 ₃₄ | 35.429 | 1340 | 1.85 |
| H ₂ O 5 ₃₃ – 4 ₀₄ | 35.471 | 725 | 1.52 |
| H ₂ O 8 ₄₅ – 7 ₃₄ | 35.669 | 1615 | 0.94 |
| H ₂ O 6 ₅₁ – 5 ₄₂ | 35.904 | 1279 | 0.60 |
| H ₂ O 6 ₅₂ – 5 ₄₁ | 35.938 | 1279 | 1.21 |
| H ₂ O 7 ₅₂ – 7 ₂₅ | 36.046 | 1525 | 0.97 |
| H ₂ O ν_2 5 ₅₀ – 4 ₄₁ | 36.161 | 3462 | 0.74 |
| H ₂ O ν_2 5 ₅₁ – 4 ₄₀ | 36.163 | 3462 | — ^a |
| H ₂ O 6 ₂₄ – 5 ₁₅ | 36.212 | 867 | 0.56 |
| H ₂ O 12 _{3,10} – 11 ₂₉ | 36.786 | 2824 | 0.40 |
| H ₂ O 7 ₄₄ – 6 ₃₃ | 37.566 | 1335 | 0.90 |
| H ₂ O 4 ₄₁ – 4 ₁₄ | 37.984 | 702 | 0.80 |
| H ₂ O 11 ₃₉ – 10 ₂₈ | 38.895 | 2439 | 0.20 |
| H ₂ O 7 ₃₄ – 7 ₀₇ | 39.045 | 1212 | 0.67 |
| H ₂ O 5 ₅₀ – 4 ₄₁ | 39.375 | 1068 | 2.31 |
| H ₂ O 5 ₅₁ – 4 ₄₀ | 39.380 | 1068 | — ^a |
| H ₂ O 6 ₄₂ – 5 ₃₃ | 39.399 | 1090 | — ^a |
| H ₂ O 12 _{2,11} – 11 _{1,10} | 40.016 | 2554 | 0.40 |
| H ₂ O 8 ₄₄ – 8 ₁₇ | 40.179 | 1628 | 0.77 |
| H ₂ O 13 _{1,13} – 12 _{0,12} | 40.188 | 2600 | — ^a |
| H ₂ O 13 _{0,13} – 12 _{1,12} | 40.189 | 2600 | — ^a |
| H ₂ O 6 ₄₃ – 5 ₃₂ | 40.337 | 1089 | 1.32 |
| H ₂ O ν_2 5 ₄₁ – 4 ₃₂ | 40.478 | 3240 | 0.90 |
| H ₂ O ν_2 5 ₄₂ – 4 ₃₁ | 40.687 | 3240 | 2.21 |
| H ₂ O 4 ₃₂ – 3 ₀₃ | 40.691 | 550 | — ^a |
| H ₂ O 6 ₃₃ – 5 ₂₄ | 40.760 | 952 | 1.17 |
| H ₂ O 11 ₂₉ – 10 ₃₈ | 40.894 | 2433 | 0.54 |
| H ₂ O 10 ₃₈ – 9 ₂₇ | 40.948 | 2081 | 0.63 |
| H ₂ O 13 _{2,12} – 13 _{1,13} | 42.427 | 2939 | 0.29 |
| H ₂ O 13 _{1,12} – 13 _{0,13} | 42.438 | 2938 | — ^a |
| H ₂ O 9 ₃₇ – 8 ₂₆ | 42.859 | 1750 | 0.79 |
| H ₂ O ν_2 5 ₂₃ – 4 ₁₄ | 43.035 | 2955 | 0.65 |
| H ₂ O 11 ₃₈ – 10 ₄₇ | 43.125 | 2609 | 0.50 |
| H ₂ O 11 _{1,10} – 10 ₂₉ | 43.250 | 2194 | 0.78 |
| H ₂ O 12 _{1,12} – 11 _{0,11} | 43.339 | 2241 | 0.24 |
| H ₂ O 12 _{0,12} – 11 _{1,11} | 43.341 | 2241 | — ^a |
| H ₂ O ν_2 7 ₃₅ – 6 ₂₄ ? | 43.713 | 3510 | 0.49 |
| H ₂ O 5 ₄₁ – 4 ₃₂ | 43.893 | 878 | 1.35 |
| H ₂ O 7 ₄₃ – 7 ₁₆ | 44.048 | 1340 | 1.15 |
| H ₂ O 5 ₄₂ – 4 ₃₁ | 44.195 | 878 | 1.14 |
| H ₂ O 8 ₃₆ – 7 ₂₅ | 44.702 | 1448 | 1.19 |

^a Line blended with previous feature. Quoted flux represents a sum over all blended lines.

^b Cross-ladder $^2\Pi_{1/2} \leftarrow ^2\Pi_{3/2}$ transitions.

TABLE 2
Results of Fabry-Perot observations of VY CMa

| Line | Rest Wavelength ^b (μm) | Upper state Energy (E/k) (K) | Line Fluxes | | Absorption line Equiv. Width W_A (km s^{-1}) | v_E ^a (km s^{-1}) |
|--|--|------------------------------------|---|---|--|--|
| | | | Emission | Absorption | | |
| | | | F_E ($10^{-18} \text{ W cm}^{-2}$) | F_A ($10^{-18} \text{ W cm}^{-2}$) | | |
| H ₂ O 7 ₂₅ – 6 ₁₆ | 29.8367 | 1126 | 2.35 | –1.94 | 11 | 22 |
| H ₂ O 4 ₄₁ – 3 ₁₂ | 31.7721 | 702 | 2.41 | –1.71 | 11 | 20 |
| H ₂ O 4 ₃₂ – 3 ₀₃ | 40.6909 | 550 | 3.69 | –2.20 | 32 | 18 |

^a Central velocity of the emission feature, relative to the LSR

^b From Toth (1991)

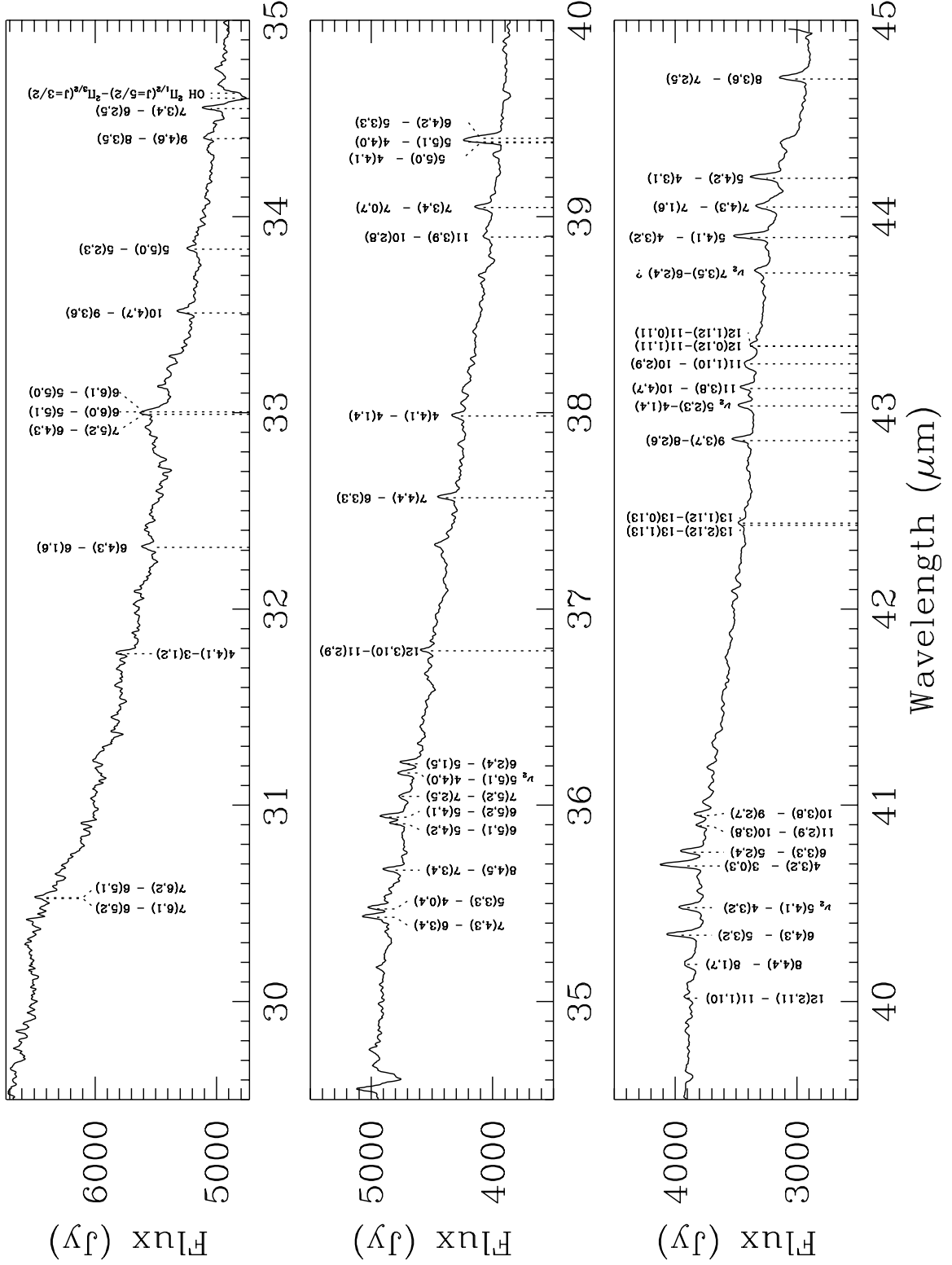


Fig. 1.— 29.5 – 45 μm SWS grating scan of VY CMa. With the exception of the OH absorption feature at 34.6 μm , all the identified features are water lines.

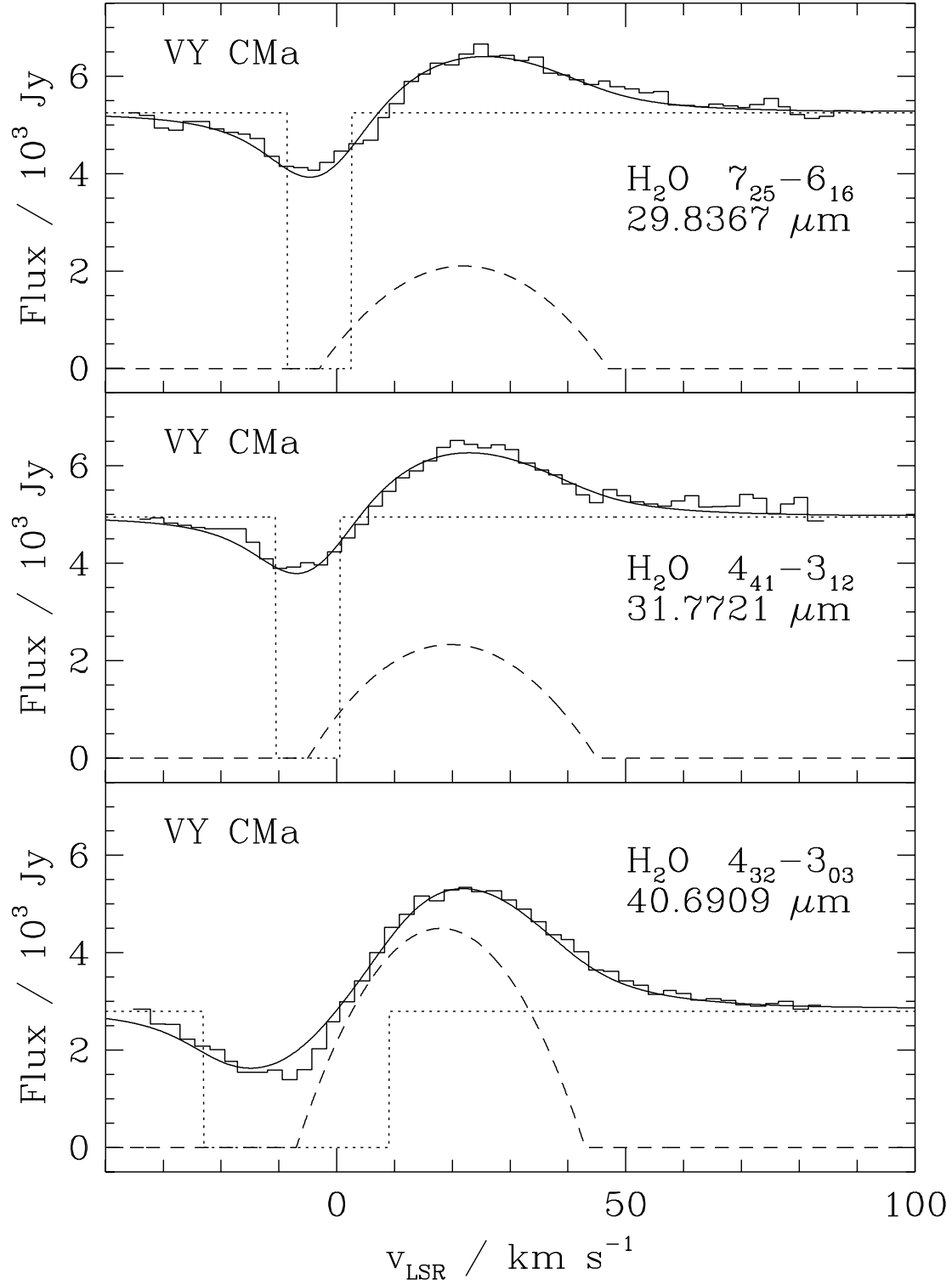


Fig. 2.— SWS Fabry-Perot spectra of three pure rotational lines of water observed towards VY CMa: the $7_{25} - 6_{16}$ line at $29.8367 \mu\text{m}$, the $4_{41} - 3_{12}$ line at $31.7721 \mu\text{m}$, and the $4_{32} - 3_{03}$ line at $40.6909 \mu\text{m}$. Solid curves show the fits described in the text, obtained by convolving the instrumental profile with the sum of the two components represented by the dotted and dashed lines.